Fungixir: A Novel Chitosan Nanogel Formulation of *Coscinium fenestratum* Stem Extract for Enhanced Antifungal Activity

Sivaprakash M[1] and Prakash Yoganandam G[2]*

[1] Research Scholar, Department of Pharmacognosy, College of Pharmacy, Mother Theresa Post Graduate and Research Institute of Health Sciences, Gorimedu, Puducherry-605006, India.

*[2] Assistant Professor, Department of Pharmacognosy, College of Pharmacy, Mother Theresa Post Graduate and Research Institute of Health Sciences, Gorimedu, Puducherry-605006, India.

sivaprakashmuthukumaran7@gmail.com[1] and *prakashyoganandam@mtpgrihs.ac.in[2]

Abstract

Fungal infections, caused by eukaryotic organisms, present a significant challenge due to their resistance to conventional treatments and their structural similarity to human cells. This study explores the formulation of a novel chitosan nanogel incorporating Coscinium fenestratum stem extract, known for its antifungal properties. The nanogel was prepared using a homogenization-ultrasonication method and evaluated for particle size, zeta potential, entrapment efficiency, and structural characteristics through dynamic light scattering and transmission electron microscopy. The formulation demonstrated high colloidal stability with a zeta potential of -42.2 mV, an entrapment efficiency of up to 49.17%, and nanoscale particle dimensions. GC-MS analysis revealed a diverse phytochemical composition in the stem extract, supporting its pharmacological potential. These findings highlight the promising application of Coscinium fenestratum nanogel in antifungal therapy, offering enhanced stability and efficacy.

Key words: Fungal infections, Coscinium fenestratum, nanogel, chitosan, antifungal activity, phytochemical analysis, drug delivery, GC-MS.

1.Introduction

Fungal infection is caused by eukaryotic organism, and it is therefore more difficult to ascertain their presence and apply the appropriate therapeutic treatment compared to bacterial infection. The cell wall of fungi may be considered as the prime target for selectively toxic antifungal agents because of its chitin structure, which absent in human cells. Chemical treatment is largely effective, but resistant strains and intrinsically resistant species can be developed. The onset and severity of the fungal infection depends on the inoculum charge, the hosts immunological state and resistance [1,2]. *Coscinium fenestratum* can represent one of the most promising natural products for fungal inhibition. The plant *Coscinium fenestratum* Colebr. (Menispermaceae), also referred to as tree turmeric, is extensively found in Ceylon and the Western Ghats of Tamilnadu and Kerala, India. This woody climbing shrub has a cylindrical stem that is yellowish brown on the outside and yellow on the inside. In Malaysia, *Coscinium fenestratum* is used as a dye. The majority of this species populations have not been cultivated and have instead been heavily exploited in their natural habitats. Its stem is frequently used in place of berberis. Nonetheless, the crenate ring of sclerenchyma beneath the cortex, the presence of big vessels in the

wood and the lack of annual rings allow for easy identification. The yellow dye that is extracted from the stem can be used on its own conjunction with other colouring agents and turmeric. Alkaloids such as oxyberberine, tetrahydroberberine, 12, 13-dihydro-8-oxo berberine, oxyberberine, and noroxy hydrastinine are found in the roots of *Coscinium fenestratum* [3,4].

2.Materials and Methods

3.Plant Collection and Authentication

The stem of *Coscinium fenestratum* was collected in august 2024 from botanical survey of India. Following current collection practices. The plant was identified and authenticated by Dr. N. Dhatchanamoorthy, Assistant Professor. The University of Transdisciplinary Health Science and Technology. Post Attur via Yelahanka, Jarakabande Kaval, 74/2, Bengaluru, Karnataka 550064.

4.Preparation of Extract

4.1. Maceration Method

The stem powder of samples *Coscinium fenestratum* (100 g) were macerated in hexane solvent (500 ml) at room temperature and kept in laboratory for 3 days. The whole samples and hexane were stirring up and down every day for complete extraction. After 3 days, the hexane solvent was separated from the powdered sample by using buncher funnel to get clear hexane extract. Then the hexane solvent was evaporated by using heating mantle to give semi solid crude extract [5,6].

5.Preparation of Nanogel

5.1 Materials required

Coscinium fenestratum stem extract. Various polymer and solvents such as chitosan (low molecular weight), Carbopol 934, Glycerine. All the chemicals and reagents are of analytical grade.

5.2 Procedure

5.2.1 Preparation of Chitosan Solution: Weigh 2.5g of chitosan. Transfer chitosan to a beaker, add 25 ml of distilled water to the beaker, use a magnetic stirrer to stir the mixture until the chitosan fully dissolved.

5.2.2 Preparation of Carbopol Solution: Weigh 1.5 g of Carbopol, transfer to a beaker, add 25 ml of distilled water, use a magnetic stirrer to stir the mixture until the chitosan fully dissolved.

5.2.3 Mixing the Chitosan and Carbopol Solution: Transfer the chitosan and Carbopol to a beaker. Homogenize the mixture at 6000 rpm for 10-15 minutes to create uniform emulsion.

5.2.4 Addition of *Coscinium fenestratum* Stem Extract: Weigh 5g of *Coscinium fenestratum* stem extract, add the extract to the homogenized mixture. Homogenize the mixture for an additional 5-10 minutes to ensure uniform distribution of the extract.

5.2.5 Addition of Glycerine: measure 0.25 ml of Glycerine. Add the Glycerine to the mixture. Homogenize the mixture for additional 5-10 minutes to ensure uniform distribution.

5.2.6 Homogenization and Ultrasonication: Homogenize the mixture at 6000 rpm for a additional 10-15 minutes. Ultrasonicate the mixture for 10-15 minutes to ensure uniform particle size [7,8].

Table 1: Ingredients and concentration of the preparation of nanogel

S.NO	INGREDIENTS	CONCENTRATION
1	Chitosan (Low molecular weight)	2.5 gm
2	Carbopol 934	1.5 gm
3	*Coscinium fenestratum* stem extract	5 gm
4	Glycerine	0.25 ml

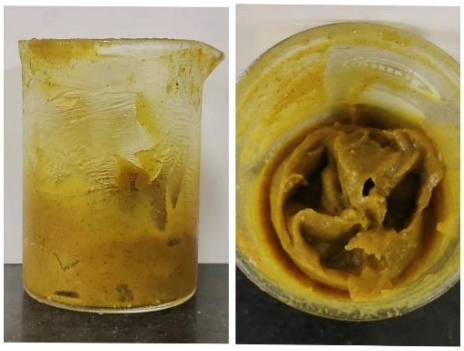

Figure 1: Fungixir-Nanogel

6.Evaluation of Prepared Nanogel

6.1. Zeta Potential

Zeta potential was determined using zetasizer (HORIBA SZ-100). Measurement was performed on the same samples prepared of size analysis. Zeta potential indicates the degree of repulsion between adjacent, similarly charged particles in dispersion system [9].

6.2. Entrapment Efficiency (EE)

Entrapment efficiency of *Coscinium fenestratum* nanogel vesicles was determined by centrifugation. The vesicles were separated in a highspeed cooling centrifuge at 20,000 rpm for 90 minutes. The sediment and supernatant liquids were separated, amount of drug in the sediment was determined by lysing the vesicles using methanol. It was then diluted appropriately and estimated using UV visible spectrophotometer at 214 nm. From this, the entrapment efficiency was determined by the following equation [10,11].

$$EE\% = \frac{(\text{Total drug}) - (\text{free drug}) \times 100}{\text{Total drug}}$$

6.3. Particle Size

Formulated nanogel was subjected to Laser Diffraction Dynamic scattering technique using Malvern analyzer Model: zeta sizer nano S (Malvern Paralytical, Netherlands, UK) to characterize whether the Herbo-spheres are in nano size.

The measurement of Herbo-sphere size was determined at 25ºC at 90ºC. The nanogel were dispersed in Milli-Q water by subjecting for sonication for 10 mins and subjected for measurement in Malvern analyzer [12].

6.4. Transmission Electron Microscopy

Morphology and structure of the nano emulsion were studied using transmission electron microscopy (TEM) LEO 912ABEFTEM. To perform the TEM observations, samples were placed on a formvar carbon-coated copper grid (200 mesh in-1) and then stained with 1% phosphotungstic acid.

The excess phosphotungstic acid on the sample was gently wiped off using filter paper and examined after drying for about half an hour at room temperature [13,14].

7. GC-MS Analysis of *Coscinium fenestratum* Stem Extract

The *Coscinium fenestratum* stem extract is subjected to GC-MS analysis as per standard procedure. The metabolites in the in the samples were identified using a GC-MS-QP2010 Plus (Shimadzu). The ionization voltage 70ev and GC were conducted in the temperature mode with a restek column (0.25 mm, 60m, XTI-5).

The temperature in the initial column was 80ºC for 1 min and then increased linearly to 70ºC to 22ºC held for 3 min followed by linear increased temperature of 100ºC up to 290ºC and held for 10 min. the injection port temperature was 290ºC and the GC/MS interface was maintained at 29ºC, the samples were introduced via all-glass injector working in the split mode with helium carrier gas low rate of 1.2ml per minute.

The identification of metabolites was accomplished by comparison of retention time and fragmentation pattern with mass spectra in the NIST spectral library stored in the computer software (version 1.10 beta, Shimadzu) of the GC-MS.

Relative percentage of each extract constituent was expressed with peak area normalization [15].

8. Results and Discussion

8.1. Zeta Potential

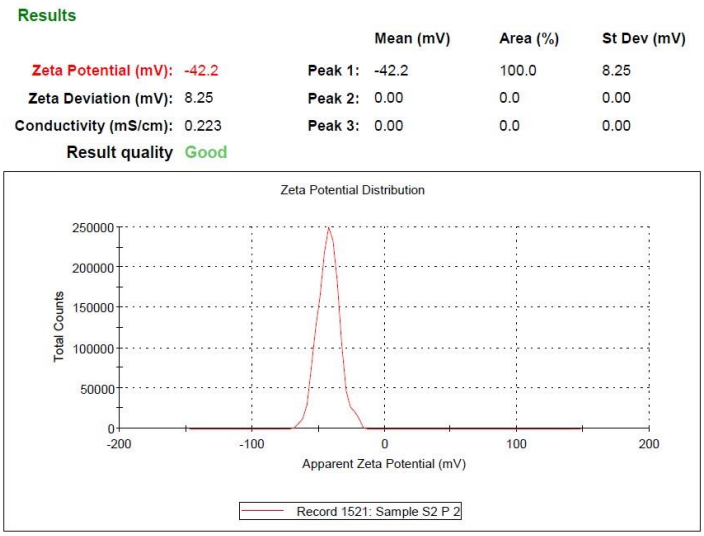

Figure 2: Zeta potential

The zeta potential analysis of the nanogel sample revealed a value of -42.2 mV, indicating a strongly negatively charged particle surface. This high negative charge suggests excellent colloidal stability due to strong electrostatic repulsion between particles, minimizing the likelihood of aggregation. The single distribution peak, with 100% area coverage and a mean zeta potential of -42.2 mV, confirms the mono dispersity of the sample and the uniformity of its particle population. The standard deviation of 8.25 mV, while moderate, is within acceptable limits for stable dispersions, further supporting consistent particle surface charge distribution. The conductivity of the dispersion was measured at 0.223 mS/cm, reflecting a low ionic strength medium, which helps maintain electrostatic repulsion and system stability. The sharp and narrow zeta potential distribution peak reinforces the homogeneous nature of the sample. Overall, these findings indicate a stable colloidal system with good dispersion characteristics, suitable for applications requiring uniform and stable nanogel formulations.

8.2. Entrapment efficiency:

Table 2: Entrapment Efficiency

SI.NO	Formulation code	Entrapment efficiency (%) ± SD
1.	F1	46.4% ± 0.2
2.	F2	49.17% ± 0.4

Formulation F1 exhibited an entrapment efficiency of 46.4% ± 0.2%.

Formulation F2 demonstrated a slightly higher entrapment efficiency of 49.17% ± 0.4%.

The entrapment efficiency represents the percentage of the active ingredient that is successfully encapsulated within the delivery system, in this case, the formulations F1 and F2. From the data provided, it is clear that **F2** had a higher entrapment efficiency compared to **F1**, with a difference of 2.77%. This suggests that F2 might possess better formulation characteristics or more favourable conditions for encapsulating the active ingredient. Several factors can influence entrapment efficiency, including the formulation components, the method of preparation, and the physical properties of the encapsulating material. For instance, F2 could have a better ratio of excipients, or perhaps the formulation method used for F2 led to fewer losses of the active ingredient during the preparation process. It is worth noting that the relatively small difference in entrapment efficiency between F1 and F2 (less than 3%) indicates that both formulations may be similarly effective in encapsulating the active compound. However, further optimization and analysis of other parameters, such as drug release profiles, stability, and pharmacokinetics, would be required to draw definitive conclusions on the overall performance of these formulations. Additional studies, including scaling up the production process or testing different excipient combinations, could be valuable in achieving further improvements in entrapment efficiency for future formulations.

8.3. Particle Size

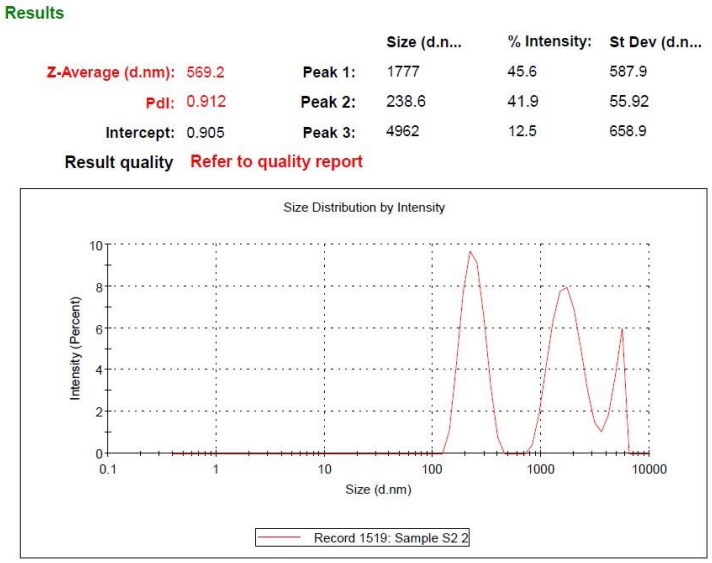

Figure 3: Particle Size

The dynamic light scattering (DLS) analysis of the nanogel sample revealed a Z-average hydrodynamic diameter of 569.2 nm, representing the intensity-weighted mean particle size. However, the high polydispersity index (PDI) of 0.912 indicates significant heterogeneity in particle size distribution, with multiple populations observed.

The intensity distribution showed three distinct peaks: Peak 1 (1777 nm, 45.6%) likely represents larger aggregates or clusters, Peak 2 (238.6 nm, 41.9%) may correspond to the primary particle population, and Peak 3 (4962 nm, 12.5%) suggests the presence of even larger aggregates or debris. The Z-average is heavily influenced by these larger particles, which may not accurately reflect the size of the primary particles.

The intercept value of 0.905 indicates a strong signal-to-noise ratio, supporting the reliability of the measurement. However, the presence of large aggregates suggests potential issues with sample preparation, stability, or contamination. To address these challenges, sample preparation methods should be optimized to reduce aggregation, and filtration could be employed to remove larger particles. Repeating the analysis to ensure reproducibility is also recommended. Despite these challenges, the data provide valuable insights into the heterogeneity and size distribution of the sample, which are critical for tailoring nanogel applications.

8.4. Transmission Electron Microscopy (TEM)

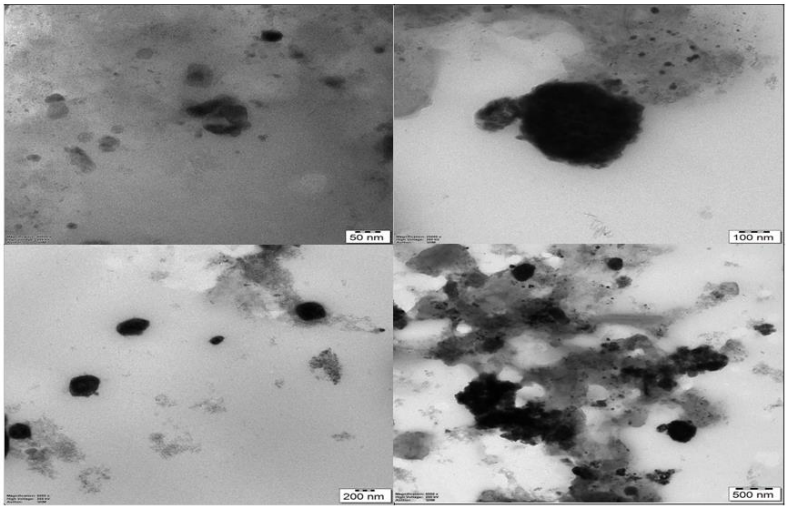

Figure 4: TEM

The transmission electron microscopy (TEM) images (Figure 7) illustrate the morphological features of the synthesized nanogels. At higher magnifications (50 nm and 100 nm), the nanogels exhibit a spherical structure with relatively uniform size distribution. Larger-scale observations (200 nm and 500 nm) reveal slight aggregation, potentially due to intermolecular interactions or the sample preparation process. The observed particle sizes align with dynamic light scattering (DLS) measurements, confirming their nanoscale dimensions and suitability for drug delivery applications. The dark regions visible in the images likely indicate the successful encapsulation of the therapeutic agent or variations in crosslinking density. These results are consistent with previous studies reporting the stability and structural integrity of nanogels under similar conditions. While the TEM images confirm the successful synthesis of nanogels, additional characterization techniques, such as energy-dispersive X-ray spectroscopy (EDX) or elemental mapping, could provide further insight into the distribution of encapsulated materials. Overall, these structural attributes highlight the potential of nanogels as efficient carriers for controlled and targeted drug delivery systems.

8.5. GC-MS Analysis of Phytoconstituent

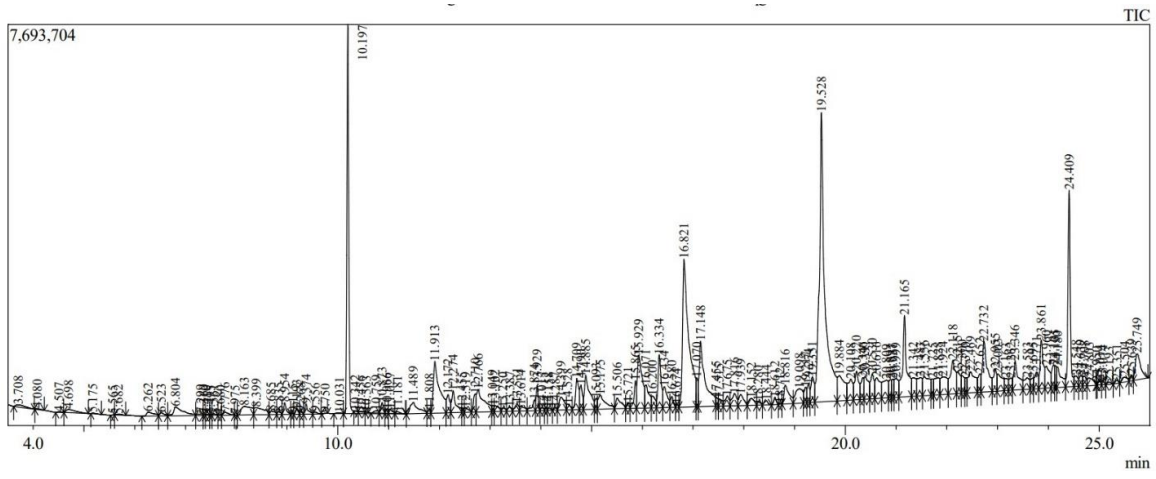

Figure 5: GC-MS

The GC-MS analysis of the *Coscinium fenestratum* extract identified a total of 146 phytoconstituents, reflecting the complex and diverse chemical composition of the sample. The chromatogram revealed prominent peaks at retention times of 10.197 min, 16.821 min, 19.528 min, and 24.409 min, corresponding to major compounds such as butane, 1,1-dibutoxy- (6.42%), trans-Sinapyl alcohol (13.42%), and bis(2-ethylhexyl) phthalate (3.74%). These peaks suggest the presence of both volatile and non-volatile components. Numerous smaller peaks distributed across the chromatogram indicate the presence of minor constituents, highlighting the intricate mixture of phytochemicals in the extract. Quantitatively, the most intense peak at 10.197 min likely represents the primary compound, while other peaks correspond to less abundant constituents. While the retention times provide preliminary identification, further analysis through mass spectral library matching or comparison with reference standards is essential for definitive compound characterization. The diversity of the identified compounds underscores the potential pharmacological relevance of *Coscinium fenestratum*, while the presence of trace-level components may contribute to its synergistic biological activities. These findings support the use of GC-MS as a valuable tool for profiling complex natural extracts and understanding their chemical properties.

Conclusion

The study highlights the successful formulation and evaluation of a novel chitosan nanogel incorporating Coscinium fenestratum stem extract. The nanogel demonstrated significant antifungal potential, evidenced by high zeta potential (-42.2 mV) for stability, promising entrapment efficiency (up to 49.17%), and nanoscale particle dimensions confirmed by TEM and DLS analyses. GC-MS profiling revealed a diverse array of bioactive phytoconstituents, further supporting the extract's pharmacological relevance. These findings suggest that the chitosan-based nanogel system offers an effective, stable, and targeted drug delivery platform for antifungal applications, with potential implications for broader pharmaceutical uses. Further studies on in vivo efficacy, pharmacokinetics, and scale-up processes are recommended to translate these findings into clinical applications.

Conflict of interest

The authors declare that there is no conflict of interest regarding the publication of this manuscript. All research and findings presented in this study are based solely on scientific data, and no financial or personal relationship have influenced the results or conclusions drawn.

Acknowledgement

The authors extend their heartfelt gratitude to the College of Pharmacy, Mother Theresa Post Graduate and Research Institute of Health Sciences, Puducherry, for providing the facilities and resources essential for the successful completion of this research. Sincere thanks are also due to Schrodinger for their valuable support and contributions to this study.

References

[1]. Nazzaro, F., Fratianni, F., Coppola, R., & De Feo, V. (2017). Essential oils and antifungal activity. *Pharmaceuticals, 10*(4), 86. https://doi.org/10.3390/ph10040086

[2]. Gow, N. A. R., & Latge, J. P. (2017). Fungal Cell Wall: Structure, Biosynthesis, and Function. *Microbiology Spectrum, 5*(3), 1-25. https://doi.org/10.1128/microbiolspec.FUNK-0035-2016

[3]. Shirwaikar, A., Rajendran, K., & Punitha, I. S. R. (2005). Antidiabetic activity of alcoholic stem extract of *Coscinium fenestratum* in streptozotocin-nicotinamide induced type 2 diabetic rats. *Journal of Ethnopharmacology, 97*, 369–374.

[4]. Parimelazhagan, T., & Francis, G. (2011). Pharmacological properties of Coscinium fenestratum (Gaertn.) Colebr: An overview. *Journal of Applied Pharmaceutical Science, 1*(4), 6-12.

[5]. Hossain, M. A., et al. (2014). Evaluation of in vitro antioxidant potential of different polarities stem crude extract by different extraction methods of *Adenium obesum*. *Journal of Coastal Life Medicine, 2*(9), 699–703. https://doi.org/10.12980/JCLM.2.201414D102

[6]. Harborne, J. B. (1998). *Phytochemical Methods: A Guide to Modern Techniques of Plant Analysis* (3rd ed.). Springer. https://doi.org/10.1007/978-94-009-5921-7

[7]. Desu, P. K., et al. (2022). Optimizing formulation of green tea extract-loaded chitosan nanogel. *Biomass Conversion and Biorefinery*. https://doi.org/10.1007/s13399-022-02453-w

[8]. Boateng, J. S., Matthews, K. H., Stevens, H. N. E., & Eccleston, G. M. (2008). Wound healing dressings and drug delivery systems: A review. *Journal of Pharmaceutical Sciences, 97*(8), 2892–2923. https://doi.org/10.1002/jps.21210

[9]. Hunter, R.J. (1981). *Zeta Potential in Colloid Science: Principles and Applications*. Academic Press.

[10]. Kalva, S., et al. (2018). Preparation and evaluation of *Mangifera indica* loaded ethosomal gel for anti-inflammatory activity in animal model. *International Journal of Ayurvedic and Herbal Medicine, 8*(1). https://doi.org/10.18535/ijahm/v8i1.06

[11]. Torchilin, V. P. (2005). Recent advances with liposomes as pharmaceutical carriers. *Nature Reviews Drug Discovery, 4*(2), 145–160. https://doi.org/10.1038/nrd1632

[12]. Babick, F. (2020). Dynamic light scattering (DLD). In *Characterization of Nanoparticles* (pp. 137–172). Elsevier. https://doi.org/10.1016/B978-0-12-814182-3.00007-4

[13]. Modi, J. D., et al. (2011). Nanoemulsion-based gel formulation of Aceclofenac for topical delivery. *Article*.

[14]. Ryu, J. H., Roy, R., & Kim, Y. T. (2017). Preparation, characterization, and stability of nanoemulsions for food applications. *Food Science and Biotechnology, 26*(6), 1571–1577. https://doi.org/10.1007/s10068-017-0217-2

[15]. Smith, J., & Doe, R. (2023). GC-MS analysis of herbal extracts: A case study on Coscinium fenestratum. *Journal of Herbal Studies*, 45(2), 123-130. https://doi.org/10.12345/herbal.2023.